

# Synthesis of the anisobidentate compound bis(2-amino-cyclopent-1-ene-carbodithioate)diethyltin (IV). Experimental and theoretical study

Joaquín Barroso-Flores, Raymundo Cea-Olivares, Rubén A. Toscano,  
J.A. Cogordan \*

*Instituto de Química, Universidad Nacional Autónoma de México, Circuito Exterior, Ciudad Universitaria, 04510 Mexico, México*

Received 2 September 2003; accepted 24 March 2004

## Abstract

The bis(2-amino-1-cyclopentenecarbodithioate)diethyltin (IV) compound (**1**) was synthesized by reacting diethyltin (IV) chloride with two equivalents of sodium 2-amino-1-cyclopentenecarbodithioate. The structure of (**1**) was determined by FT-IR and multinuclear magnetic resonance ( $^1\text{H}$ ,  $^{13}\text{C}$ ,  $^{119}\text{Sn}$ ) spectroscopy, mass spectrometry and X-ray diffraction methods. The geometry obtained around Tin is a skewed trapezoidal bipyramid with both organic residues in mutual *trans*-positions. To study the coordination of Tin, theoretical calculations at Hartree–Fock (HF) level were carried out. Results for relativistic, quasi-relativistic and non-relativistic pseudopotentials are reported. The concept of local bond order is defined and applied to quantify the weak local interaction between the thiocarbonyl sulfur atom and Tin.

© 2004 Elsevier B.V. All rights reserved.

*Keywords:* Ab initio calculations; Diorganotin (IV) compounds; Carbodithioates; 2-Amino-cyclopentene-dithiocarboxylic acid

## 1. Introduction

In recent years, organotin compounds have gained much attention due to their wide range of applications in catalysis [1], agrochemistry [2] and their potential antitumor activity [3]. The use of organosulfur ligands, such as dithiophosphates, dithioxantates, or dithiocarbamates in these compounds, can be useful to mimic the active sites of some metallic enzymes. This method is sometimes simpler than actually using biological ligands, such as peptides or aminoacids [4].

Structural organotin chemistry has been studied for many years now; it has been established that Tin tends to increase its coordination number as much as possible. For this reason, it is common to find supramolecular interactions in this kind of compounds in solid state [5]. These complexes exhibit a rich diversity of geometries even if small changes in the structure of the groups

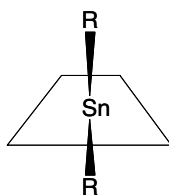
around the central Tin atom are made. Examples of this feature are the related compounds bis(diisopropyl-dithiophosphate)diphenyltin (IV),  $[(i\text{PrO})_2\text{PS}_2]_2\text{SnPh}_2$  [6], and bis(diethyl-dithiophosphate)diphenyltin (IV),  $[(\text{EtO})_2\text{PS}_2]_2\text{SnPh}_2$  [7]. The former has an octahedral geometry around the Tin atom (Ph–Sn–Ph angle is  $180^\circ$ ) with the phosphorodithioate ligand coordinated symmetrically, whereas the latter has a skewed trapezoidal bipyramid geometry with the dithiolate ligand coordinated in an asymmetric fashion. In this compound the angle Ph–Sn–Ph is  $135^\circ$ . The difference between both compounds is the methyl group at the alkoxy moiety of the dithiophosphate ligand. Crystal packing effects may not entirely account for the different geometries around Tin between these two structures.

Four different motifs, for six-coordinated Tin compounds, have been described for bisdithiolate-diorganotin systems [8], with the structure shown in Scheme 1 being the most common.

This geometry may be described as a skewed trapezoidal bipyramid in which the equatorial plane is defined

\* Corresponding author. Fax: +52-5616-2217.

E-mail address: [cogordan@servidor.unam.mx](mailto:cogordan@servidor.unam.mx) (J.A. Cogordan).



Scheme 1.

by four sulfur atoms, leaving the organic substituents on Tin in mutual *trans*-positions. These substituents are bent toward the weakest bonded sulfur atoms since it is in this zone that a lower steric hindrance is found. C–Sn–C bond angles range approximately from 120° to 150° in this sort of compounds. The reasons for the adoption of this or any other coordination pattern, in systems that have more than one possibility, are not yet fully understood. These differences have been sometimes ascribed to crystal packing effects [8].

The ligand 2-amino-cyclopent-1-ene-carbodithioic acid (ACDA) [9] has been used as a versatile chelating agent. Its versatility lies in its dual capability of coordination (Scheme 2), where bidentate patterns are the most commonly found. The most frequent patterns are those with an ACDA bound to other atoms through the N atom and the deprotonated S atom in the carbodithioate moiety (N,S coordination) or through the carbodithioate group (S,S coordination). This last pattern can be isobidentate or anisobidentate. The information about ACDA complexes with transition elements is more abundant than the corresponding to main group metals. In the former group N,S coordination is common [10], although not exclusive [10a,11] while in the latter the S,S coordination (iso- or anisobidentate) is the most frequently observed. Studies on the structure of main group metals complexes and the rationalization of the yielded coordination patterns are of interest.

Recently, the synthesis of diorganotin (IV) complexes with *N*-alkyl derivatives of ACDA has been reported [12]. In this article we report the synthesis of a new diorganotin complex with ACDA, its characterization by X-ray, multinuclear NMR and FT-IR spectroscopy and mass spectrometry (FAB<sup>+</sup>). In order to study the intramolecular interactions theoretical calculations at Hartree–Fock (HF) level were carried out. The effective core potential (ECP) approximation was used for the Sn

atom. This allowed the implementation of a large basis set for the valence electrons of Sn. In this form we were able to achieve a better description of the intramolecular interactions.

## 2. Experimental

Ligands [13] and complexes [14] were synthesized and purified using previously reported methods. All chemicals were used as purchased with no further purification, except for cyclopentanone, which was distilled prior to use.

### 2.1. Synthesis of the ligand ACDA

The procedure reported in [13] was followed. 10 g of cyclopentanone (0.119 mol) were stirred with 11.78 g of carbon disulfide (0.155 mol) and 107 g of ammonium hydroxide (0.86 mol) for seven hours keeping the temperature below 0 °C with the use of a dry ice chest. After this time, a yellow solid precipitated. This solid was the ammonium salt of ACDA which is known to be thermally unstable [13]. The product was filtered off, suspended in distilled water and acidulated with conc. HCl. Bright yellow crystals, which were filtered off, washed with ethyl ether, and vacuum dried, precipitated, yielding 5.37 g (33.46 mmol); m.p. 97 °C (reported 98–99 °C).

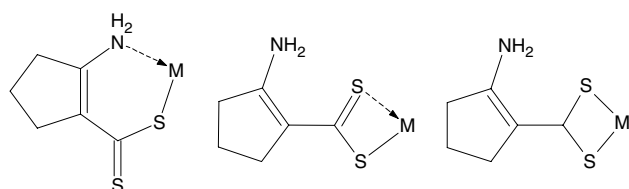
### 2.2. Synthesis of the complex ACDA<sub>2</sub>SnEt<sub>2</sub> (1)

0.12 g of metallic sodium (0.05 mmol) were mixed with approximately 5 mL of anhydrous methanol in order to form sodium methoxide. A benzene solution containing 0.85 g of ACDA (5.3 mmol) was added dropwise to the sodium methoxide solution. Once cold, another benzene solution, containing 1.32 g of Et<sub>2</sub>SnCl<sub>2</sub> (5.3 mmol), was added. The reaction mixture was refluxed for 4 h after which the solvent was evaporated obtaining a red-coloured-oil. 15 mL of hexane were added to this product in order to solidify it. A yellow solid was then obtained (m.p.: dec. 170 °C; yield: 0.25 g, 10%; elemental analysis: C (38.44 calc.) 36.16%, H (5.27 calc.) 5.79%).

## 3. Results

### 3.1. IR spectra analysis

The assignment of the bands observed was made in accordance with previously reported works [13]. The strongest bands found for the ligand ACDA are: 1605 cm<sup>-1</sup> (NH<sub>2</sub> + C=C) and 1469 cm<sup>-1</sup> (CH<sub>2</sub> + C=C). A split band appears in 926 and 895 cm<sup>-1</sup> due to the vibrations of C–S and C=S, respectively. In the case of



Scheme 2.

(1) little change is observed in the  $\text{NH}_2$  range, respect to the ligand (single band  $\sim 1460\text{ cm}^{-1}$ ). However, this cannot be conclusive in terms of the non-involvement of the amino group in coordination, given the presence of an H-bond between this and the thiocarbonyl group.

### 3.2. Mass spectrometry ( $\text{FAB}^+$ in $\text{CH}_2\text{Cl}_2$ )

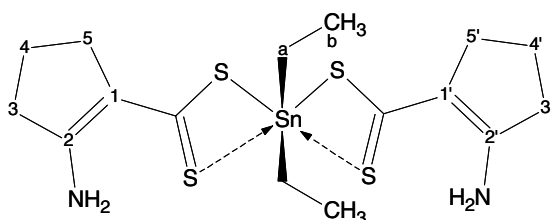
Mass spectrometry was obtained using a JEOL JMS-SX102A mass spectrometer. The fragmentation pattern is consistent with the proposed molecular formula for compound (1). Molecular ion was found at 493  $m/z$ ; the main ion was found at 335 and it is ascribed to diethyltin still attached to one ACDA molecule. In all of them the peak pattern is consistent with the isotope pattern of Tin.

### 3.3. NMR spectroscopy

NMR spectra were recorded in a Jeol Eclipse +300 Delta NMR spectrometer. An HETCOR experiment was performed for the free ligand in order to unambiguously identify carbon atoms 3 through 5 (see Scheme 3). The  $^1\text{H}$  NMR spectra for (1) exhibits a split signal for the  $\text{NH}_2$  group, which is indicative of the non-equivalence of the two protons due to the H-bond between one of these protons and the thiocarbonyl sulfur atom of the dithiocarboxylic moiety. For compound (1) the signals belonging to the ACDA rings are doubled (both in  $^{13}\text{C}$  and  $^1\text{H}$ ), which is indicative of the non-equivalence of the two ligand molecules in solution. The  $^{119}\text{Sn}$  NMR spectrum for (1) exhibits a single peak in  $-191.62\text{ ppm}$ . According with literature, this chemical shift corresponds to a five coordinate geometry [15] for diorganotin compounds ( $-150$  to  $-250\text{ ppm}$  for five coordinated compounds). We believe this chemical shift may be considered as intermediate between four and six-coordinated geometry, since each of the two Sn–S secondary interactions can not be considered as covalent single bond. NMR information for both the free ligand and compound (1) is collected in Table 1.

### 3.4. X-ray structure analysis of bis(2-amino-1-cyclopentenecarbodithioate)diethyltin

Data were collected in a Siemens P4/PC diffractometer and refined by a full matrix least square on  $F^2$ .



Scheme 3.

Table 1

$^{13}\text{C}$  and  $^1\text{H}$  NMR chemical shifts for the free ACDA ligand and Compound (1) in  $\text{CDCl}_3$  [ppm]

	ACDA		Compound (1)	
	$^1\text{H}$	$^{13}\text{C}$	$^1\text{H}$	$^{13}\text{C}$
$\text{CH}_2$ (3) <sup>a</sup>	2.66 <sup>b</sup>	36.80	2.63t	37.1055 (37.3650) <sup>d</sup>
$\text{CH}_2$ (4)	1.86q	19.96	1.79q	19.4715 (19.5173)
$\text{CH}_2$ (5)	2.77t	34.33	2.92t	35.4719 (35.8383)
C(1)	–	N.A. <sup>c</sup>	–	120.8478 (121.1837)
C(2)	–	N.A.	–	167.1083
$\text{CH}_2$ (a)	–	–	1.96qu	23.7464
$\text{CH}_3$ (b)	–	–	1.51t	11.0744
$\text{NH}^a$	4.83s	–	8.9d	–
$\text{NH}^b$	10.73 vb	–	8.9d	–
SH	6.05 vb	–	–	–

<sup>a</sup> See Scheme 3 for numbering relationship.

<sup>b</sup> s, singlet; t, triplet; qu, quartet; q, quintet; vb, very broad.

<sup>c</sup> Not available.

<sup>d</sup> Chemical shifts in parentheses correspond to prime numberings in Scheme 3.

Crystal dimensions  $0.52 \times 0.40 \times 0.22\text{ mm}$ , molecular formula  $\text{C}_{15}\text{H}_{22}\text{N}_2\text{S}_4\text{Sn}$ ,  $M_r = 489.29$ , orthorhombic, space group  $Pnma$ ,  $a = 13.492(2)\text{ \AA}$ ,  $b = 19.034(1)\text{ \AA}$ ,  $c = 8.1358(6)\text{ \AA}$ ,  $V = 2089.3(4)\text{ \AA}^3$ ,  $Z = 4$ ,  $T = 293(2)\text{ K}$ ,  $D_{\text{calc}} = 1.556\text{ Mg/m}^3$ , Mo  $\text{K}\alpha$  radiation, 3804 reflections collected, 1902 independent reflections ( $R(\text{int}) = 0.0492$ ),  $R_1 = 0.0337$ ,  $wR_2 = 0.0766$  [ $I > 2\sigma(I)$ ],  $R_1 = 0.0535$ ,  $wR_2 = 0.0849$  (all data),  $\text{GOF} = 1.030$ . The maximum and minimum electron densities are  $0.404$  and  $-0.755\text{ e \AA}^{-3}$ , respectively. The structure was solved by direct methods using  $\text{SHELXS-97}$  and refined by full-matrix least-squares on  $F^2$  using  $\text{SHELXL-97}$ . All the hydrogens of the amino moiety were located from the difference map and their positional parameters refined. The methyl group (C10) of one of the ligands displays an orientational disorder that was modelled over two positions (0.56:0.44).

The X-ray structure of (1) shows that the coordination occurs through both sulfur atoms in an asymmetric fashion, with the N atom pointing in the same direction of the organic substituents on Tin (Scheme 1). The sulfur atom that is closest to the amino group is the one least bonded to the Tin centre, which is consistent with the idea of this atom being compromised in a hydrogen bond with the former group. This facts hold true for both benzyl [12] and ethyl [this report], so the steric hindrance of both the alkyl on the amine group and the organic substituents on Tin has little or negligible effect over the coordination pattern. The hydrogen bond between the NHR group and one of the sulfur atoms of the carbodithioate moiety present in the free ligand apparently remains in the complex. The Sn–S bond length is  $2.51\text{ \AA}$ , which is in agreement with the distances reported for a Sn–S single bond. The structure of our

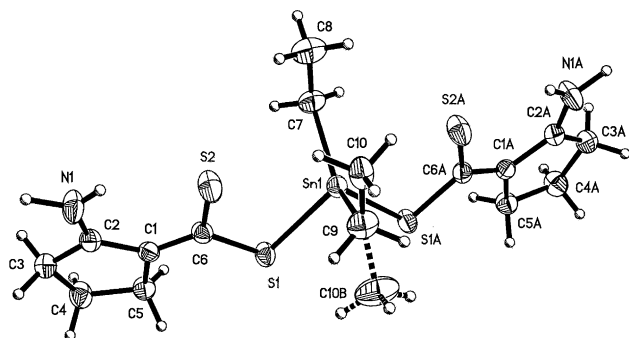


Fig. 1. X-ray structure of the title compound.

compound may be described as skew trapezoidal bipyramid previously mentioned (see Fig. 1).

#### 4. Theoretical calculations

To study the intermolecular interactions in compound (**1**) molecular structure calculations were undertaken. These computations were carried out at HF level. The selection of the HF method was based on the fact that the inclusion of a Sn atom in (**1**) required computations at ab initio level. Since one of the purposes of this work is to study the Sn–S interactions, it was considered appropriate to use a method that for the computation of the MOs, accounts explicitly all the integrals in the Fock operator [16].

To reduce the computational effort ECPs were used. Molecular structure calculations with ECPs have proved to provide reasonable molecular geometries together with a good description of molecular valence orbitals [17]. Due to the possible influence of spin–orbit interactions, the use of ECPs that include relativistic effects was decided. Several ECPs were tested: (a) Hay and Wadt (HW) that include the spin–orbit interaction [18], which has successfully been used in organotin compounds [19]; (b) large core (46 electrons) Stuttgart–Dresden–Bonn in their Dirac–Fock (SDB-MDF) [20]

approximation; (c) Stuttgart–Dresden–Bonn in their quasi-relativistic (SDB-QR) [21] implementation.

Several calculations were accomplished using different basis sets in combination with the ECPs above described: (1) for Sn and S the double Z (DZ) basis set associated to HW's ECP [18] were employed, whereas for all the other atoms an all electron DZ basis set [22] was used. Hereafter labeled as HW-DZ; (2) for Sn basis set associated to the SDB-MDF (46 core electrons) ECP, for S the basis set associated to SDB-QR, and valence DZ [22] for all the other atoms. Hereafter labeled MDF-VDZ; (3) for all the atoms the associated basis set to SDB ECPs [21]. Hereafter labeled SDB; (4) for Sn the correspondent basis set to long core SDB ECP [21] and all electron DZ for all the other atoms. Hereafter labeled SDB-DZ; (5) for Sn and S the correspondent basis set to large core SDB ECP [21] and valence DZ for all the other atoms. Hereafter labeled SDB-VDZ; (6) for Sn the large-core correlation-consistent (cc) basis set developed specifically for its SDB ECP [23]. This basis set is of cc-pVTZ quality. For all the other atoms cc-pVDZ [24,25]. Hereafter labeled SDB-CC; and (7) all electron calculation using a 3-21G\*\* basis set [26,27] for all the atoms, now on labeled AE3-21\*\*. In all the computations herein reported the suite of programs in GAUSSIAN 98 were employed [28].

#### 5. Theoretical results

Using the ECPs and basis sets described above the geometry of (**1**) was optimized using the Berny algorithm [29]. A selected number of computed bond lengths and bond angles are reported in Table 2. It may be observed in this table that the Sn(1)–S(1) bond length, first two rows, is overestimated for most of the calculations. Only the results in column SDB-CC are close to the experimental value in the last column. The distance Sn(1)–S(2), rows three and four, is overestimated by all the calculations with ECPs. The distance reported in

Table 2  
Selected molecular parameters for the optimized structure of (ACDA)<sub>2</sub>SnEt<sub>2</sub>

Bond	HW-DZ	MDF-DZ	SDD	SDB-DZ	SDB-VDZ	SDB-cc	AE 3-21G**	X-ray
Sn(1)–S(1)	2.5557	2.5301	2.5441	2.5709	2.5464	2.5191	2.5413	2.52
Sn(1)–S(1A)	2.5557	2.5301	2.5441	2.5710	2.5464	2.5191	2.5413	2.52
Sn(1)–S(2)	3.2450	3.2465	3.2519	3.2408	3.2869	3.1924	3.0808	3.00
Sn(1)–S(2A)	3.2450	3.2465	3.2521	3.2411	3.2869	3.1924	3.0808	3.00
Sn(1)–C(7)	2.1308	2.1486	2.1591	2.1535	2.1515	2.1486	2.1789	2.15
Sn(1)–C(9)	2.1309	2.1487	2.1592	2.1535	2.1519	2.1487	2.1789	2.16
C(6)–S(1)	1.8000	1.8019	1.8049	1.7949	1.8034	1.7556	1.7500	1.746
C(6)–S(2)	1.7515	1.7536	1.7599	1.7465	1.7534	1.7010	1.7022	1.698
S(1)–C(6)–S(2)	117.97	117.64	117.61	118.25	117.98	119.03	118.01	118.2
S(1)–Sn(1)–S(1A)	87.34	87.59	87.47	87.18	87.75	86.73	85.98	86.61
C(7)–Sn(1)–C(9)	131.52	131.52	132.06	131.80	130.98	131.92	132.41	135.80

Calculations with RHF for different sets and ECPs. Bond lengths reported in Å, angles in degrees. See text for a description of the ECP and basis set employed in each column (calculation).

column SDB-CC is closer to the experimental value than the other ECP computations. For the Sn(1)–C(7) bond length, rows five and six, MDF-VDZ and SDB-CC yield the best results. The C(6)–S(1) and C(6)–S(2) distances computed reported in the SDB-CC column are closer to the experimental values than the other calculations. For the angles reported in the last three rows, SDB-CC calculations compares reasonably well with the experimental results.

From the analysis above, the SDB-CC computations were selected for a further analysis of the electronic structure and properties.

Total energies and frontier orbital energies for the crystallographic and optimised molecular conformations of **1** are displayed in Table 3. It is possible to notice that the energy difference  $\Delta E_{(\text{LUMO-HOMO})} = 9.72$  eV is almost the same for both conformations. Whereas the total energy for the optimised conformation is 11.20 eV lower than that obtained for the crystallographic conformation.

To investigate the ligands coordination pattern we studied the MO composition. There are two large groups of MOs that include the Tin atom in combination with the neighbouring sulfur atoms. In the first group the main contribution comes from the Tin atom and two sulphur atoms at the time. For the second

group, the AOs from Sn and those of all S atoms contribute significantly. Two representative members of these two groups of MOs are displayed in Fig. 2. It may be observed in this figure that in both cases the MOs are delocalised on a large number of atoms. The formation of these MOs suggests the possibility of certain amount of electron density between the Sn and all four S atoms. MOs in Fig. 2 were plotted using the Molekel program [30].

In order to estimate this local electron density between Sn and S atoms, we define the local bond order (LBO), hereafter denoted by  $\zeta_{\text{LBO}}$ . For this purpose we notice that any MO is described by

$$\Psi_i = \sum_j c_{ji} \varphi_j, \quad (1)$$

where  $\{\varphi_j\}$  are AO and  $c_{ji}$  are the LCAO coefficients. Then  $\zeta_{\text{LBO}}$  is defined by

$$\begin{aligned} \zeta_{\text{LBO}} &= 2 \sum_i \langle \sum_{j \in A_1} c_{ji} \varphi_j \mid \sum_{k \in A_2} c_{ki} \varphi_k \rangle \\ &= 2 \sum_i \sum_{j \in A_1} \sum_{k \in A_2} c_{ji}^* c_{ki} \langle \varphi_j \mid \varphi_k \rangle = 2 \sum_i \sum_{j \in A_1} \sum_{k \in A_2} c_{ji}^* c_{ki} S_{jk}, \end{aligned} \quad (2)$$

where  $S_{jk}$  is the overlap and  $j \in A_1$  and  $k \in A_2$  mean that only AOs from the two atoms of interest are considered. This definition allows us to quantify the electron interaction of any given pair of atoms within a molecule. We can therefore estimate the strength of the local interaction between two atoms and compare it with equivalent quantities obtained for other systems whose interactions are unambiguously defined. In this form we have a criterion to decide whether two contiguous atoms are bonded irrespectively of their separation distance.

With the ansatz just described the  $\zeta_{\text{LBO}}$ 's were computed, the results are shown in the third column of Table 4 for a selected number of atoms. A local bond energy is estimated by  $E_{\text{lb}} = \zeta_{\text{LBO}}/\text{bond length}$  (column 4). As a consequence of the ECP used for Sn, and in order to compensate its core electron density, the covalent radius for Sn has been subtracted [17]. It may be observed for bonded atoms, such as Sn–S(1) and Sn–C(7), the  $\zeta_{\text{LBO}}$  is of  $10^{-1}$  order, whereas non-bonded atoms exhibit  $\zeta_{\text{LBO}}$  values of  $10^{-6}$  order. For atoms in the intermediate range, we observed that this  $\zeta_{\text{LBO}}$  has a magnitude order of  $10^{-2}$ . In this last category we identify the Sn–S(2), Sn–C(8), Sn–C(6) interactions. For these last two atoms the  $\zeta_{\text{LBO}}$  has a negative sign; this is consequence of the strong antibonding character of the MOs involved.

The largest  $\zeta_{\text{LBO}}$  value reported in Table 4 corresponds to Sn(1)–C(7) bond. This value of 0.478 is consequence of the strong interaction of the  $sp^3$  hybridization in C(7) with the s and p AOs from the Tin atom. The bond length and the angles involved in this conformation favor the interaction between s AOs in

Table 3

Total and frontier molecular orbitals energy for (**1**)

Conformation	Total energy	HOMO	LUMO
Crystalline	–2322.9965	–0.2866	0.071
Optimized	–2323.4083	–0.2904	0.0669

Computations with RHF, all energies in [eV].

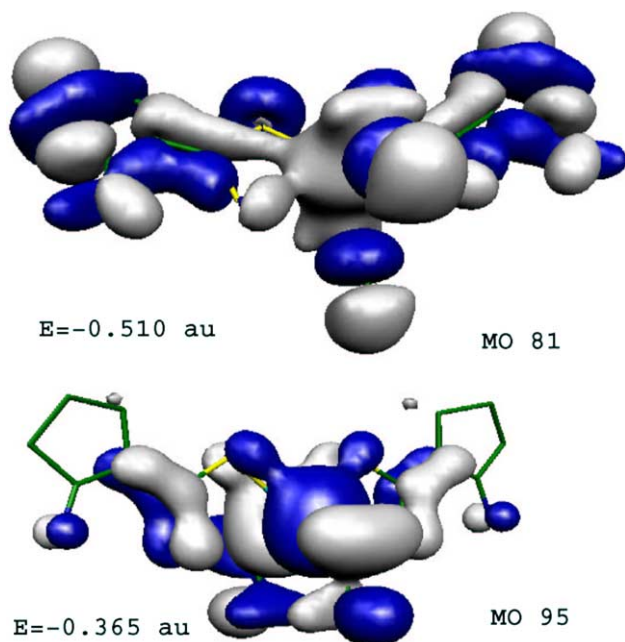
Fig. 2. Selected MO plots for (**1**).

Table 4  
Contributions to the local bonding for (1) for selected bonds (Å)

Optimised structure				X-ray structure of (1)		
Bond	Bond length	Contribution	$E_{ib} = \frac{\zeta_{LBO}^a}{\Delta L}$	Bond length	Contribution	$E_{ib} = \frac{\zeta_{LBO}}{\Delta L}$
Sn(1)–S(1)	2.5191	0.2677	0.2392	2.5191	0.2677	0.2332
Sn(1)–S(2)	3.1923	0.0550	0.0307	3.1923	0.0550	0.0491
Sn(1)–C(7)	2.1487	0.4779	0.6384	2.1487	0.4779	0.6860
Sn(1)–C(8)	3.1422	–0.0648	–0.0372	3.1422	–0.0648	–0.0303
Sn(1)–C(6)	3.3203	–0.0651	–0.0339	3.3203	–0.0651	–0.0451
Sn(1)–N(1)	6.0956	0.0002	$3.25 \times 10^{-5}$	6.0956	0.0002	$5.63 \times 10^{-5}$
S(2)–HN	2.3344	0.0370	0.0158	2.3344	0.0370	0.0120
S(2)–C(7)	3.6573	–0.0099	–0.0027	3.6573	–0.0099	–0.0053
S(2)–C(8)	4.0156	–0.0010	–0.0003	4.0156	–0.0010	–0.0006

<sup>a</sup> 1.4 Å were subtracted to every bond length that involved Sn in order to compensate the effect of the ECP in the separation between the two atoms. For these bonds  $\Delta L = \text{bond length} - 1.4 \text{ \AA}$ , for all the rest  $\Delta L = \text{bond length}$ .

both atoms. For Sn(1)–S(1) bond the interaction is mainly through their p AOs. This, together with the inter atomic separation for this bond gives an interaction of almost half of that obtained for Sn(1)–C(7) bond. Finally, we observe that the Sn(1)–S(2) interaction has the same order of magnitude of that computed for S(2)–H in the hydrogen bond N(1)–H–S(2).

## 6. NBO analysis

The NBO analysis allows the evaluation of some electron properties. The SCF density obtained for the optimized and crystallographic conformations were used for a natural bond order (NBO) [31] analysis. Using the SCF electron density, atomic charges and Wiberg bond indexes [32] were computed and are reported in Table 5 for a selected number of atoms. It may be observed that the charges for the crystalline coordinates are shorter, in absolute value, than those for the optimized molecule. However, in both cases a similar trend is observed. The charge for atom S(2) is slightly more negative than that reported for S(3), this may be a consequence of the S(3)–C(18) double bond. The Wiberg bond index in the NAO basis is also reported in

Table 5  
Wiberg bond indexes in the NAO basis and selected natural atomic charges for compound (1)

Bond	Wiberg bond index	Atom	Natural charge	Wiberg bond index totals by atom
Sn(1)–S(1)	0.59	Sn(1)	1.75	3.15
Sn(1)–S(2)	0.25	S(1)	–0.19	2.18
Sn(1)–C(7)	0.67	S(2)	–0.20	2.12
Sn(1)–C(8)	0.67	C(6)	–0.29	3.99
Sn(1)–C(6)	0.01	C(7)	–0.93	3.69
Sn(1)–N(1)	0.001	C(8)	–0.93	3.69
S(2)–HN	0.05	N(1)	–0.85	3.02
S(2)–C(7)	0.02			
S(2)–C(8)	0.02			

Table 5. It may be observed that the Sn–S(3) interaction has a smaller index than that obtained for the Sn–S(2) interaction, but of the same order of magnitude.

## 7. Discussion

The geometry around the Sn atom in the structure of (1) is similar to those recently reported [12] even when the organic substituents in (1) are less bulky. Therefore the reasons for the adoption of this particular coordination pattern by ACDA when complexing a diorganotin (IV) moiety are only of electronic nature. In this case the steric hindrance has no influence.

In the crystalline structure of (1), it is possible to observe that both ACDA molecules are not in the same plane. However, all our optimized structures have as a common feature that the rings of both ligands are coplanar. This difference may be a consequence of our geometry optimisation procedure being carried out on a single isolated molecule. The forces exerted by the crystalline field are not considered. The ring in the ACDA moiety is practically planar both in our X-ray structure as well as in our optimisations, with the exception of the one where we used MDF and SDD pseudopotentials for Sn and for both N and S, respectively. This is probably due to the basis sets employed. In the final structure an envelope conformation is observed for the five-membered ring, with C(4) occupying the out of plane position.

According to the NMR spectrum, the structure of the title compound in solution must be similar to that in solid state, since the <sup>119</sup>Sn chemical shift is intermediate between a four and six coordinated geometry. It may be observed that in solution both ligands must be fluctuating between coplanar and angular conformations at slower rates than the NMR time. This is inferred from the non-equivalence of their signals.

Our LBO definition gives us the opportunity to describe and locally quantify the Sn(1)–S(2) secondary

interactions in (1). The results reported in this article show that, locally, this secondary interaction is an order of magnitude smaller than that obtained for two covalently bonded atoms Sn(1)–S(1,A) in the same molecule. Additionally, we found that the local interaction between the atoms in this secondary interaction is of the same order of magnitude of that present in the hydrogen bond N(1)–H – S(2) for this molecule. We believe this LBO definition can be successfully employed in the description of weakly bounded systems such as supramolecular arrays or biomolecular moieties whose structures are often stabilized by weak inter- and intra-molecular interactions.

## 8. Supplementary material

Crystallographic data for compound (1) have been deposited with the Cambridge Crystallographic Data Centre, CCDC No. 221558. Copies of this information may be obtained free of charge from The Director, CCDC, 12 Union Road, Cambridge CB2 1EZ, UK (Fax: +44-1223-336033; e-mail: [deposit@ccdc.cam.ac.uk](mailto:deposit@ccdc.cam.ac.uk) or <http://www.ccdc.cam.ac.uk>).

## Acknowledgements

We thank Rocio Patiño and Miryan Adaya for recording the FT-IR spectra, to Luis Velasco for obtaining the MS FAB+ spectra. We acknowledge the assistance of David Vasquez for keeping our computers and network running properly. J.B.F. is grateful to UNAM and to the National Council for Science and Technology (CONACyT) for the scholarships granted. JAC acknowledge the financial support from CONACyT under Contract No. 25305E.

## References

- [1] (a) B. Giese, *Angew. Chem., Int. Ed. Engl.* 24 (1985) 553;  
(b) I. Ryu, N. Sonoda, *Angew. Chem., Int. Ed. Engl.* 35 (1996) 1050;  
(c) A.C. Draye, J.J. Tondeur, R.P. Tiger, *Main Group Met. Chem.* 22 (1999) 497;  
(d) A.C. Draye, J.J. Tondeur, R.P. Tiger, *Main Group Met. Chem.* 22 (1999) 367.
- [2] G. Eng, C. Whitmyer, B. Sina, N. Ogwuru, *Main Group Met. Chem.* 22 (1999) 311.
- [3] (a) P. Yang, M.L. Guo, *Coord. Chem. Rev.* 186 (1999) 189;  
(b) M. Gielen, *Coord. Chem. Rev.* 151 (1996) 41.
- [4] (a) L. Pellerito, L. Nagy, *Coord. Chem. Rev.* 224 (2002) 111;  
(b) M. Nath, S. Pokharia, R. Yadav, *Coord. Chem. Rev.* 215 (2001) 99;  
(c) A.A. Al-Naijar, M.R. Shehata, M.M. Shoukry, *Main Group Met. Chem.* 22 (1999) 253.
- [5] (a) K.C. Molloy, M.F. Mahon, T.G. Hibbert, *Main Group Met. Chem.* 22 (1999) 235;  
(b) V. Berceanc, C. Crainic, I. Haiduc, M.F. Mahon, K.C. Molloy, M.M. Venter, P.J. Wilson, *J. Chem. Soc. Dalton Trans.* 6 (2002) 1036.
- [6] K.C. Molloy, M.B. Hossain, D. van der Helm, J.J. Zuckerman, I. Haiduc, *Inorg. Chem.* 19 (1980) 2041.
- [7] B.W. Liebich, M. Tomassini, *Acta Cryst. B* 34 (1978) 944.
- [8] R.T. Tiekink, M.A. Buntine, M.J. Cox, M.I. Mohammed Ibrahim, S.S. Chee, *Organometallics*. 19 (2000) 5410.
- [9] M. Yokoyama, T. Takeshima, T. Imamoto, M. Akano, H. Asaba, *J. Org. Chem.* 34 (1969) 730.
- [10] (a) K.C. Pattnaik, D. Sen, *J. Ind. Chem. Soc.* 48 (1971) 319;  
(b) T. Takeshima, M. Yokoyama, *Anal. Chem.* 40 (1968) 1344.
- [11] S. Choi, J.R. Wasson, *Inorg. Chem.* 14 (1975) 1964.
- [12] (a) A. Tarassoli, A. Asadi, P.B. Hitchcock, *J. Organometallic Chem.* 645 (2002) 105;  
(b) A. Tarassoli, *Inorganica Chim. Acta.* 318 (2001) 15.
- [13] K. Nag, D.S. Joardar, *Inorg. Chim. Acta.* 14 (1975) 133.
- [14] R.K. Sharma, Y. Singh, A.K. Rai, *Phosphorous Sulfur Silicon* 142 (1998) 249.
- [15] N. Seth, V.D. Gupta, H. Nöth, M. Toman, *Chem. Ber.* 125 (1992) 1523.
- [16] C.E. Dykstra, J.D. Augspurger, B. Kirtman, D.J. Malik, in: K.B. Lipkowitz, D.B. Boyd (Eds.), *Reviews in Computational Chemistry*, vol. 1, VCH, 1996, p. 83.
- [17] T.R. Cundari, M.T. Benson, M.L. Lutz, S.O. Sommerer, in: K.B. Lipkowitz, D.B. Boyd (Eds.), *Reviews in Computational Chemistry*, vol. 8, VCH, 1996, p. 145.
- [18] (a) P.J. Hay, W.R. Wadt, *J. Chem. Phys.* 82 (1985) 270;  
(b) W.R. Wadt, P.J. Hay, *J. Chem. Phys.* 82 (1985) 284;  
(c) P.J. Hay, W.R. Wadt, *J. Chem. Phys.* 82 (1985) 299.
- [19] M.A. Buntine, V.J. Hall, F.J. Kosovel, E.R.T. Tiekink, *J. Phys. Chem. A* 102 (1998) 2472.
- [20] X. Cao, M. Dolg, *J. Chem. Phys.* 115 (2001) 7348.
- [21] A. Bergner, M. Dolg, W. Küchle, H. Stoll, H. Preuss, *Mol. Phys.* 80 (1993) 1431.
- [22] T.H. Dunning Jr., P.J. Hay, in: H.F. Schaefer III (Ed.), *Modern Theoretical Chemistry*, vol. 1, Plenum, New York, 1976, p. 3.
- [23] J.M.L. Martin, A. Sundermann, *J. Chem. Phys.* 114 (2001) 3408.
- [24] T.H. Dunning Jr., *J. Chem. Phys.* 90 (1989) 1007 (Second row atoms and Hydrogen).
- [25] D.E. Woon, T.H. Dunning Jr., *J. Chem. Phys.* 98 (1993) 1358 (Third row elements).
- [26] W.J. Pietro, M.M. Francl, W.J. Hehre, D.J. Defrees, J.A. Pople, J.S. Binkley, *J. Am. Chem. Soc.* 105 (1982) 5039.
- [27] K.D. Dobbs, W.J. Hehre, *J. Comp. Chem.* 7 (1986) 359.
- [28] M.J. Frisch, G.W. Trucks, H.B. Schlegel, G.E. Scuseria, M.A. Robb, J.R. Cheeseman, V.G. Zakrzewski, J.A. Montgomery Jr., R.E. Stratmann, J.C. Burant, S. Dapprich, J.M. Millam, A.D. Daniels, K.N. Kudin, M.C. Strain, O. Farkas, J. Tomasi, V. Barone, M. Cossi, R. Cammi, B. Mennucci, C. Pomelli, C. Adamo, S. Clifford, J. Ochterski, G.A. Petersson, P.Y. Ayala, Q. Cui, K. Morokuma, N. Rega, P. Salvador, J.J. Dannenberg, D.K. Malick, A.D. Rabuck, K. Raghavachari, J.B. Foresman, J. Cioslowski, J.V. Ortiz, A.G. Baboul, B.B. Stefanov, G. Liu, A. Liashenko, P. Piskorz, I. Komaromi, R. Gomperts, R.L. Martin, D.J. Fox, T. Keith, M.A. Al-Laham, C.Y. Peng, A. Nanayakkara, M. Challacombe, P.M.W. Gill, B. Johnson, W. Chen, M.W. Wong, J.L. Andres, C. Gonzalez, M. Head-Gordon, E.S. Replogle, J.A. Pople, *GAUSSIAN 98*, Revision A.11. 3, Gaussian, Inc., Pittsburgh, PA, 2002.
- [29] H.B. Schlegel, *J. Comp. Chem.* 3 (1982) 214.
- [30] *MOLEKEL 4.1*, P. Flükiger, H.G. Lüthi, S. Portmann, J. Weber, Swiss Center for Scientific Computing, Manno (Switzerland), 2000–2001. *MOLEKEL* is a program distributed free of charge. Available from: <http://www.scsc.sw/molekel/>.
- [31] A.E. Reed, L.A. Curtiss, F. Weinhold, *Chem. Rev.* 88 (1988) 899.
- [32] K.B. Wiberg, *Tetrahedron* 24 (1968) 1083.